

## Effects of Spin Speed on the Photoelectrochemical Properties of Fe<sub>2</sub>O<sub>3</sub> Thin Films

Kan-Rong Lee<sup>1</sup>, Ya-Ping Hsu<sup>1</sup>, Jeng-Kuei Chang<sup>1,2</sup>, Sheng-Wei Lee<sup>2</sup>, Chung-Jen Tseng<sup>1,\*</sup>,  
Jason Shian-Ching Jang<sup>1,2</sup>

<sup>1</sup>Department of Mechanical Engineering, National Central University, Jhongli, Taiwan

<sup>2</sup>Institute of Materials Science and Engineering, National Central University, Jhongli, Taiwan

\*E-mail: [cjtseng@ncu.edu.tw](mailto:cjtseng@ncu.edu.tw)

Received: 4 September 2014 / Accepted: 23 September 2014 / Published: 28 October 2014

---

In this work, we report the effects of spin speed on structure and photoelectrochemical properties of Fe<sub>2</sub>O<sub>3</sub> thin films. The Fe<sub>2</sub>O<sub>3</sub> thin films were prepared by sol-gel method and spin coated on fluorine-tin-oxide coated glass substrate. The material properties were examined by *X-ray diffraction (XRD)*, field emission scanning electron microscopy (FESEM), and optical spectroscopy. The photoelectrochemical characteristics were investigated at room temperature. It was demonstrated that heat treatment in air atmosphere greatly enhanced the *XRD* peak intensity and photocurrent density. Results of *XRD* show that  $\alpha$ -Fe<sub>2</sub>O<sub>3</sub> can be obtained using 500 °C annealing in air. The direct band gaps of the samples obtained from reflectance and transmittance spectra measurement are found to vary from 2.0 to 2.05 eV. The 5000-rpm sample has the maximum photocurrent density of 0.5 mA/cm<sup>2</sup> (at 0.5 V vs. Ag/AgCl) under a 300 W Xe lamp system. These good photoelectrochemical results and stability of the Fe<sub>2</sub>O<sub>3</sub> thin film warrants further investigation for broader applications in the future.

---

**Keywords:** Iron oxide, Sol-gel, Photoelectrochemical method, Water splitting, Hydrogen production

### 1. INTRODUCTION

In various green energies, hydrogen has been recognized as highly efficient due to their high thermodynamic efficiency. Hydrogen can be produced by many methods from a variety of sources. One promising method is the photoelectrochemical (PEC) splitting of water using solar irradiation [1-7]. In 1972, Fujishima and Honda [8] reported producing hydrogen by splitting of water using TiO<sub>2</sub> electrode. Since then, many semiconductors, such as  $\alpha$ -Fe<sub>2</sub>O<sub>3</sub>, WO<sub>3</sub> [9], and ZnO [10], have attracted much attention.

Hematite ( $\alpha\text{-Fe}_2\text{O}_3$ ) has emerged as a promising photo-electrode material due to its significant light absorption, chemical stability in aqueous environments, and ample abundance. The energy band gap of  $\alpha\text{-Fe}_2\text{O}_3$  is about 2.1 eV, enabling better utilization of the solar energy for water splitting than using  $\text{TiO}_2$  electrodes. In 1978, Kennedy and Frese [11] reported good stability of  $\alpha\text{-Fe}_2\text{O}_3$  electrode in alkaline solution. However the energy conversion efficiency of  $\alpha\text{-Fe}_2\text{O}_3$  is not very good due to its high electron-hole recombination rate. In order to improve the conversion efficiency, many proposed to add a small amount of a third element, such as Mg [12], Cu, Zn [13], Al [14], Pt [15], Ti and Sn [16]. In addition, Luo et al. [17] used  $\text{WO}_3/\alpha\text{-Fe}_2\text{O}_3$  composite thin film to enhance photocurrent density. Later, Wang et al. [18] prepared  $\text{SrTiO}_3/\text{Fe}_2\text{O}_3$  composite photoanode by spin-coating.

Although doping additional element may be an effective way to increase the conversion efficiency, there are rooms for improvement by re-examining process parameters. In this work, we investigate the effects of spin speed of spin coating, annealing environment and annealing temperature on the structure and photoelectrochemical properties of  $\alpha\text{-Fe}_2\text{O}_3$  thin films.

## 2. EXPERIMENTAL METHODS

### 2.1. Preparation of electrodes

Thin films of  $\alpha\text{-Fe}_2\text{O}_3$  were prepared by sol-gel spin-coating on fluorine doped tin oxide (FTO) glasses. The substrates were cleaned with alcohol, acetone, and isopropanol before each coating. The precursor of reaction solvent was  $\text{FeCl}_3 \cdot 6\text{H}_2\text{O}$  (0.5 M), adjusted to a volume ratio of 36:1:1 mixture of  $(\text{CH}_3)_2\text{CHOH}$ ,  $\text{HOCH}_2\text{CH}_2\text{OH}$ , and  $\text{HCl}$ . The speed of spin was controlled at 3000, 5000 and 7000 rpm for 20 seconds. All films were heated at  $250^\circ\text{C}$  for evaporation of solvents, and then heat treated at  $500^\circ\text{C}$  for 2 hours in air and oxygen, respectively.

### 2.2. Characterization of electrodes

The morphology of samples was observed using field emission scanning electron microscope (FE-SEM, JEOL, JSM-7401F). The crystal structure of samples was measured using an X-ray diffractometer (XRD, Shimadzu, XRD-6000 X) with  $\text{CuK}\alpha$  ( $\lambda = 1.5418 \text{ \AA}$ ) radiation in the  $2\theta$  range of  $20\text{-}65^\circ$ . The scan rate was  $5^\circ/\text{min}$ .

The optical characteristic of samples was measured by UV-Vis spectrophotometer with an integrating sphere (JASCO, V-670) and resolution of 1 nm. After obtaining the transmittance,  $T$  and reflectance,  $R$  of the  $\text{Fe}_2\text{O}_3$  films, the absorption coefficient ( $\alpha$ ) can be calculated from [19]:

$$\alpha = \frac{1}{d} \left( \ln \frac{1-R}{T} \right) \quad (1)$$

where  $d$  (nm) is the thickness of the film. The energy band gap,  $E_g$  can then be determined from the following equation [20]:

$$\alpha h\nu = A(h\nu - E_g)^n \quad (2)$$

where  $h\nu$  is the incident photo energy,  $A$  is a constant.  $n = 1/2$  indicates direct allowed transition, and  $n = 2$  indicates indirect allowed transition.

The PEC performance of the samples were measured in a standard three-electrode system consisting of a  $\alpha\text{-Fe}_2\text{O}_3$  sample as the working electrode, a Pt plate ( $\sim 1 \times 1 \text{ cm}^2$ ) as the counter electrode, Ag/AgCl as the reference electrode, and  $\text{Na}_2\text{S}$  (0.35 M) and  $\text{K}_2\text{SO}_3$  (0.25 M) as the aqueous electrolyte (pH value = 13). The electrolyte was prepared using double deionized water and degassed by purging with nitrogen gas before each experiment. The photocurrent density of films, as a function of applied voltage, was varied from - 0.5 V to + 1.0 V vs. Ag/AgCl reference electrode (scan rate = 0.05 V/s) and using a 300 W solar simulator (Newport-Oriel Instruments, Model: 91160-1000) with AM 1.5 filter as a light source.

### 3. RESULTS AND DISCUSSION

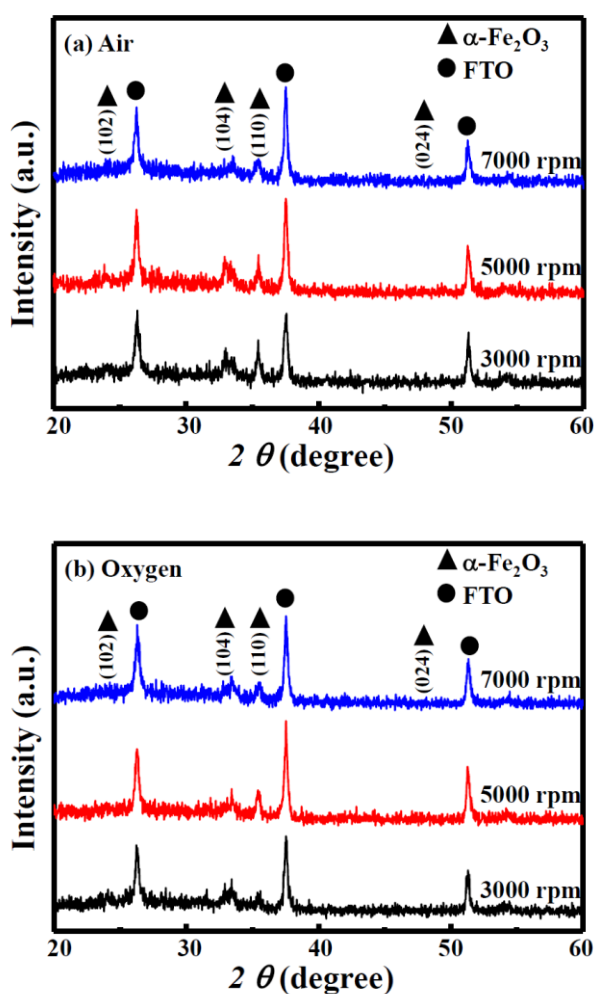
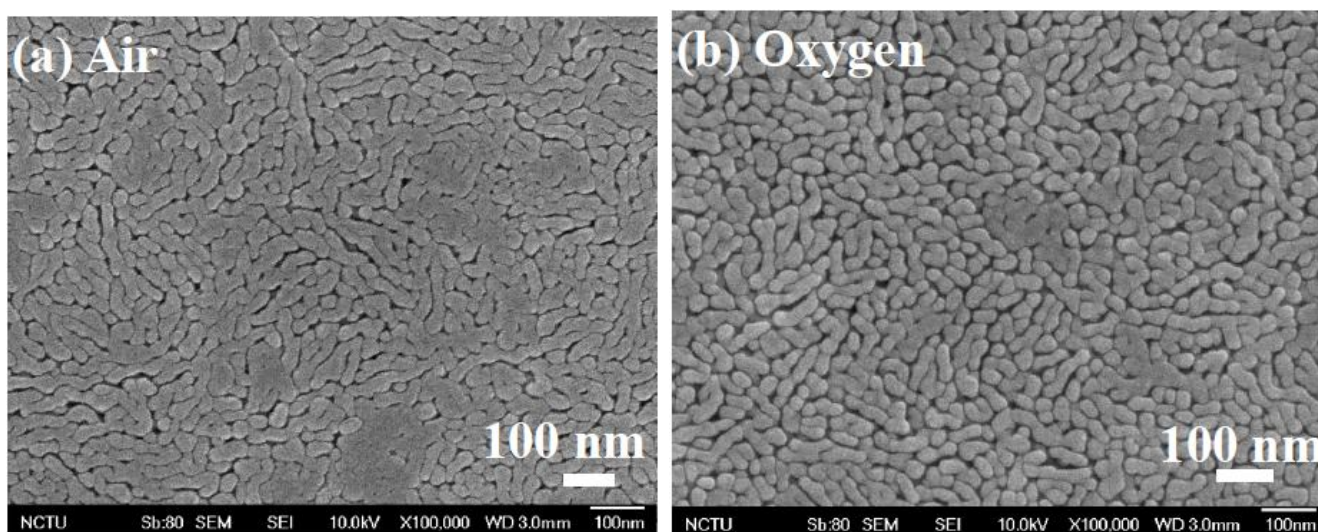


**Figure 1.** X-ray diffraction results of  $\alpha\text{-Fe}_2\text{O}_3$  thin films prepared with different spin speed and heat treated at 500 °C in (a) air, and (b) oxygen.

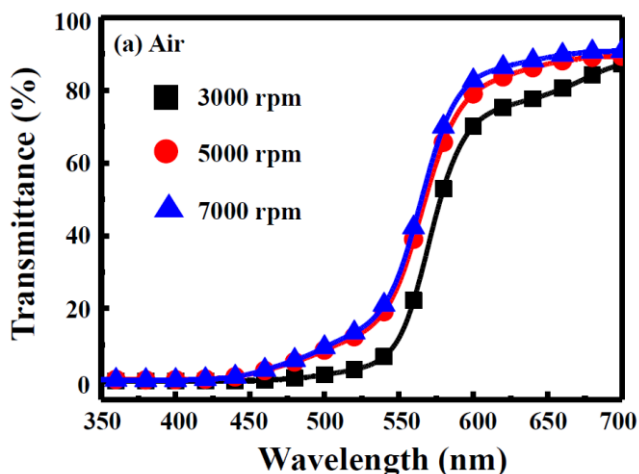
Figure 1 shows the results of XRD for the different spin speed (3000, 5000 and 7000 rpm) heat treated in air and in oxygen at 500 °C. All the oxides can be identified as a pure  $\alpha$ -Fe<sub>2</sub>O<sub>3</sub> structure, showing four major diffraction signals, namely those from the (102), (104), (110), and (024) planes. Comparing the samples annealed in air and in oxygen, the main peak (110) in air is stronger than that in oxygen. The grain size can be obtained with the aid of Scherrer's equation

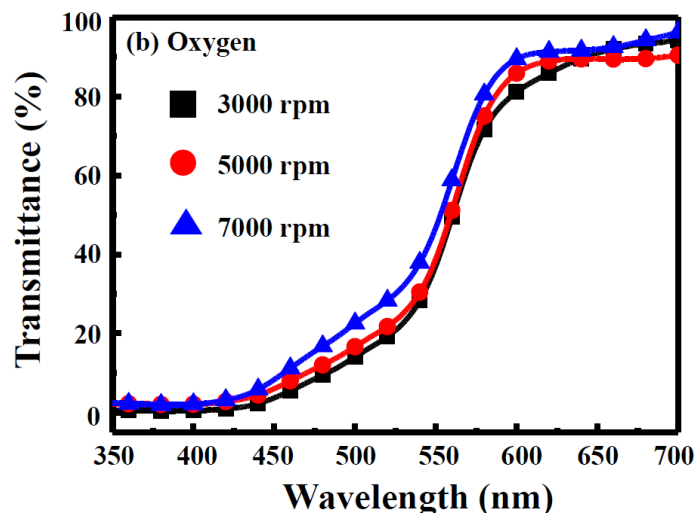
$$D = \frac{0.9\lambda}{\beta \cos \theta} \tag{1}$$

where  $D$ ,  $\lambda$ ,  $\beta$ , and  $\theta$  are the mean grain size, X-ray wavelength, the full width at half maximum (FWHM) of the diffraction peak, and the Bragg angle, respectively. From this equation, the grain size of all samples calculated from the (110) peak was found to be 26 nm. Consistent results were obtained by FE-SEM. The FE-SEM images for the  $\alpha$ -Fe<sub>2</sub>O<sub>3</sub> thin films heat treated in air and in oxygen with spin speed at 5000 rpm are shown in Fig. 2. They show uniform worm-like grains and resemble Lian et al.'s results [21].

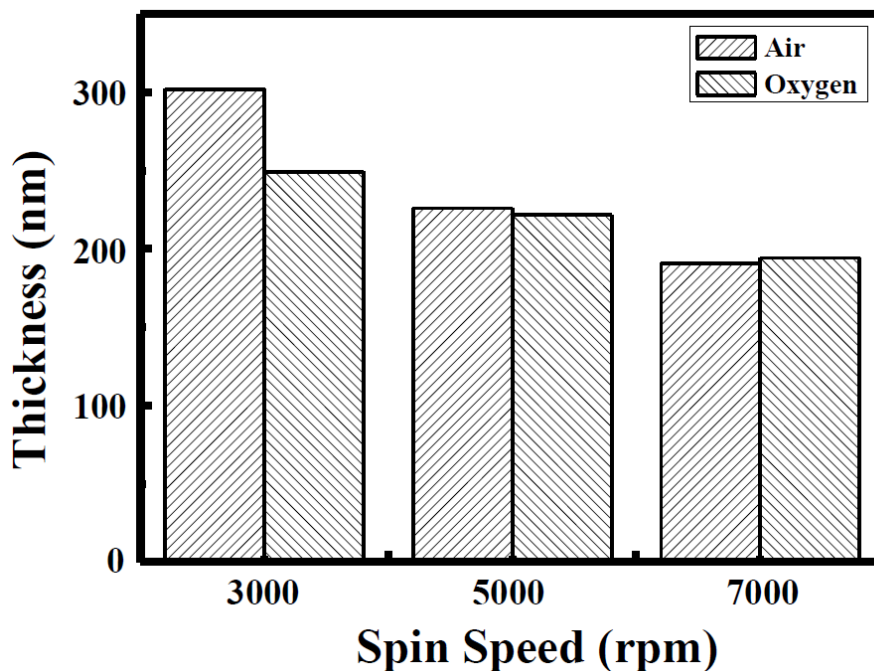


**Figure 2.** FE-SEM images of  $\alpha$ -Fe<sub>2</sub>O<sub>3</sub> thin films prepared with different spin speed and heat treated at 500 °C in (a) air, and (b) oxygen.



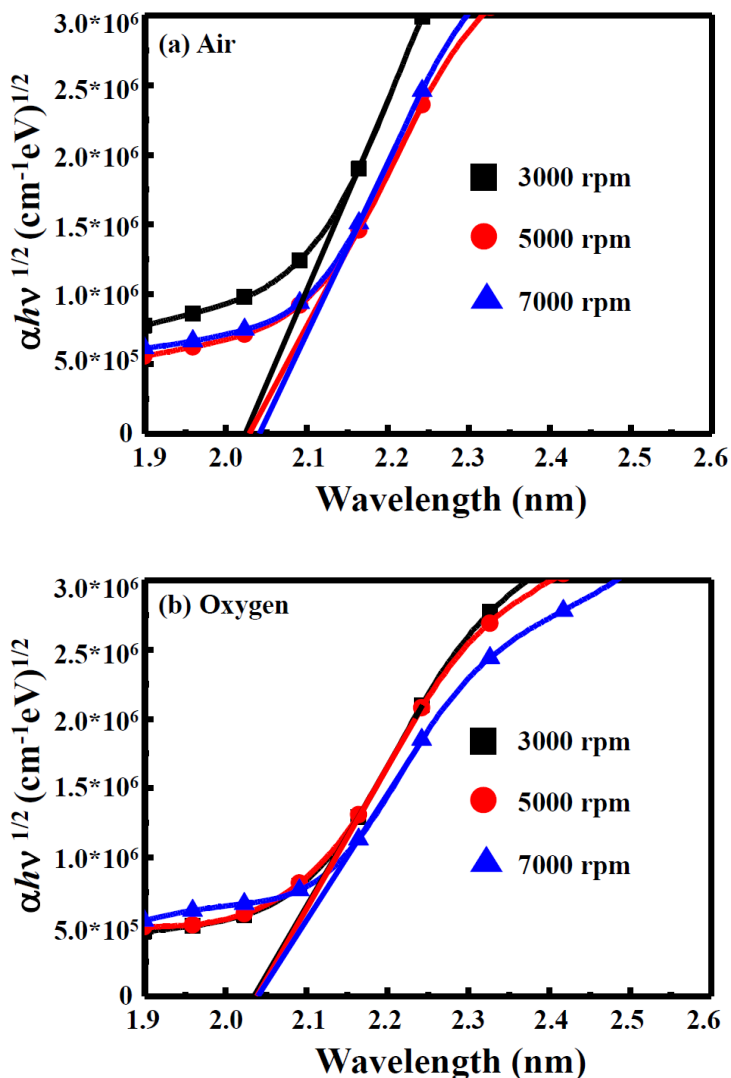


**Figure 3.** Transmittance spectra of  $\alpha$ -Fe<sub>2</sub>O<sub>3</sub> thin films prepared with different spin speed and heat treated at 500 °C in (a) air, and (b) oxygen.

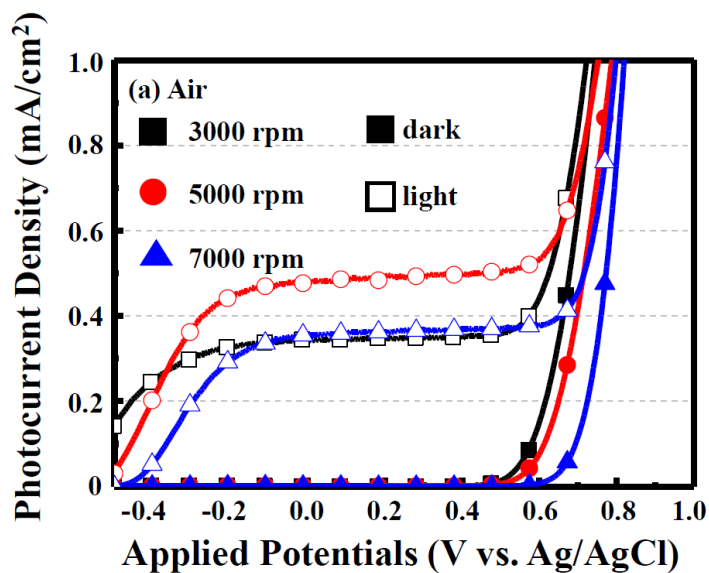


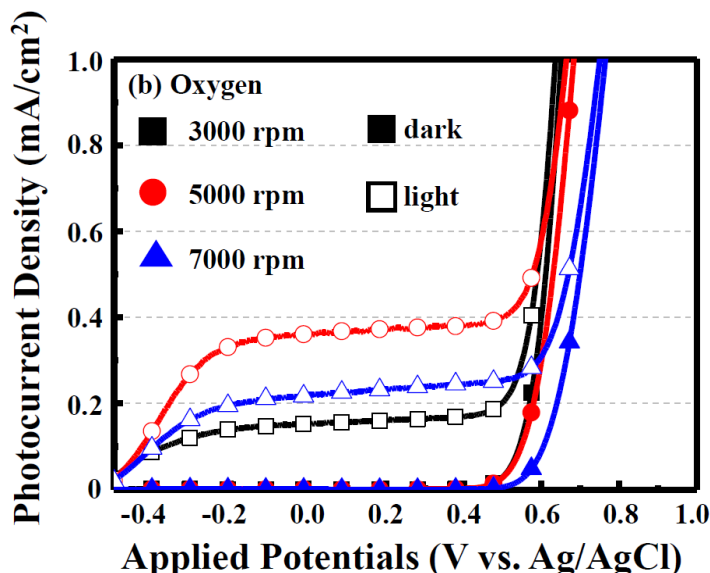
**Figure 4.** Thickness of the  $\alpha$ -Fe<sub>2</sub>O<sub>3</sub> thin film samples prepared with different spin speed.

Figure 3 shows transmittance spectra measured by ultraviolet-visible spectrometer for samples with different annealing atmosphere. These films are highly transparent in the range from 580 nm to 700 nm. Similar result was also observed by Ismail et al [22]. The transmittance increases with increasing spin speed due to decreasing thickness (Fig. 4). The  $(\alpha h\nu)^{1/2}$  vs.  $h\nu$  plot is presented in Fig. 5. The band gap of the samples can be obtained from extrapolating the linear portions of the respective curve to  $(\alpha h\nu)^{1/2} = 0$ . The band gap of  $\alpha$ -Fe<sub>2</sub>O<sub>3</sub> films heat treated in different ambient was found to be in the range of 2.0-2.05 eV.



**Figure 5.** Plots of  $(\alpha h\nu)^{1/2}$  vs.  $h\nu$  for samples prepared with different spin speed and heat treated at 500 °C in (a) air, and (b) oxygen.





**Figure 6.** Photocurrent density - applied voltages plots of samples under 300 W solar simulators (AM 1.5G, 100 mW/cm<sup>2</sup>, 25°C), (a) air, and (b) oxygen.

Figure 6 demonstrates photocurrent density as a function of applied potential (vs. Ag/AgCl) of the different spin speed and heat treatment ambient samples in 0.5 M K<sub>2</sub>SO<sub>3</sub> + NaOH (pH = 13) electrolyte solution. In general, the photocurrent density is higher for samples heat treated in air than in oxygen. For the spin speed at 3000 rpm, the photocurrent density for heat treated in air and in oxygen is 0.35 and 0.18 mA/cm<sup>2</sup>, respectively. As the spin speed is increased to 5000 rpm, the photocurrent density increases for both heat treated in air and in oxygen. However, the photocurrent density decreases as the spin speed is further increased to 7000 rpm. There appears to exist a best spin speed for the process. The photocurrent density depends on film thickness. As film thickness increases, more light can be absorbed. However, thicker film also results in higher electron-hole pair recombination. Therefore, there exist a best thickness that corresponds to a best spin speed.

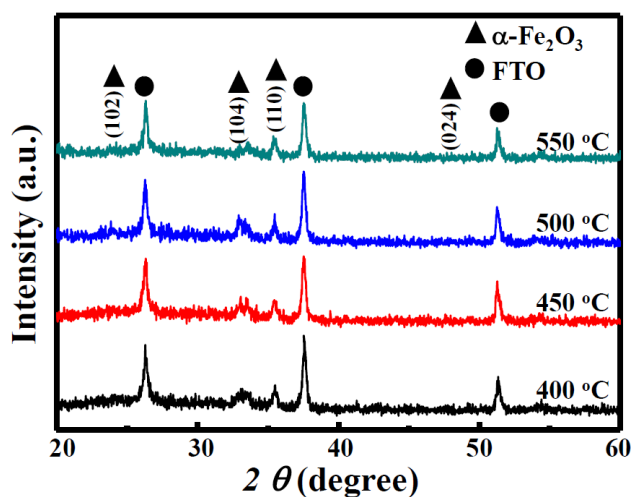


**Figure 7.** X-ray diffraction results of  $\alpha$ -Fe<sub>2</sub>O<sub>3</sub> thin films for different heat treatment temperatures.

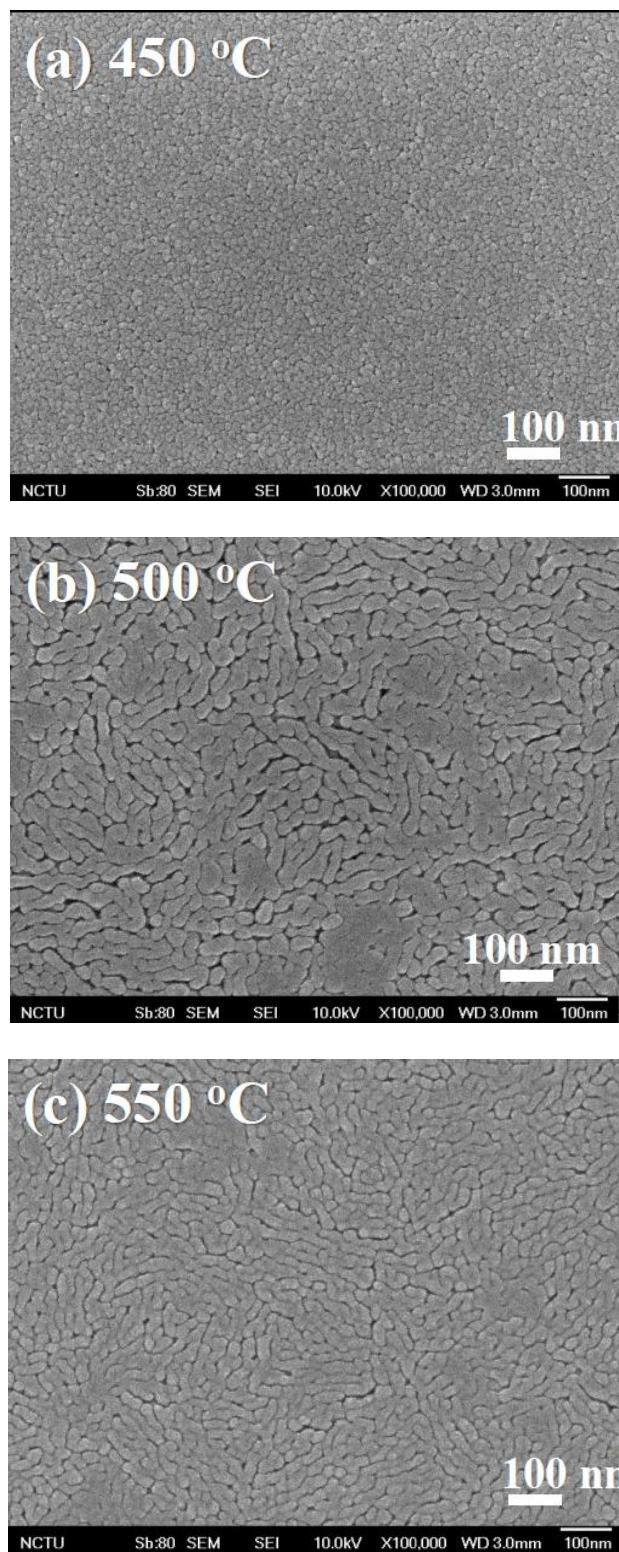


**Figure 8.** FE-SEM images of  $\alpha$ -Fe<sub>2</sub>O<sub>3</sub> thin films for different heat treatment temperatures, (a) 450 °C, (b) 500 °C and (c) 550 °C.

Figure 7 shows the XRD diffraction patterns for Fe<sub>2</sub>O<sub>3</sub> thin films prepared with a spin speed of 5000 rpm and heat treated in air at different temperatures. For heat treatment temperatures of 400°C and 450°C, the intensity of the major peak (110) is not strong. This means that the driving force for

$\text{Fe}_2\text{O}_3$  crystallization was not enough at 400°C and 450°C. Increasing the heat treatment temperature to 500°C, the major peak (110) becomes stronger and shows narrower full width at half maximum height (FWHM). However, the intensity decreases and FWHM widens as heat treatment temperature is further increased to 550°C.

The corresponding SEM images are shown in Fig. 8. As heat treatment temperature is increased from 450°C to 500°C, the grain grows obviously, confirming XRD results. However, as heat treatment temperature is further increased to 550°C, the grain size decreased slightly. In order to investigate this abnormal trend, we heating the FTO substrate to 500°C and 550°C. The surface morphology of the heat treated FTO substrate is shown in Fig. 9. While the FTO film remains flat for the 500°C case, it was clearly destroyed for the sample treated at 550 °C. The destroyed surface may lead to the abnormal grain size decrease.

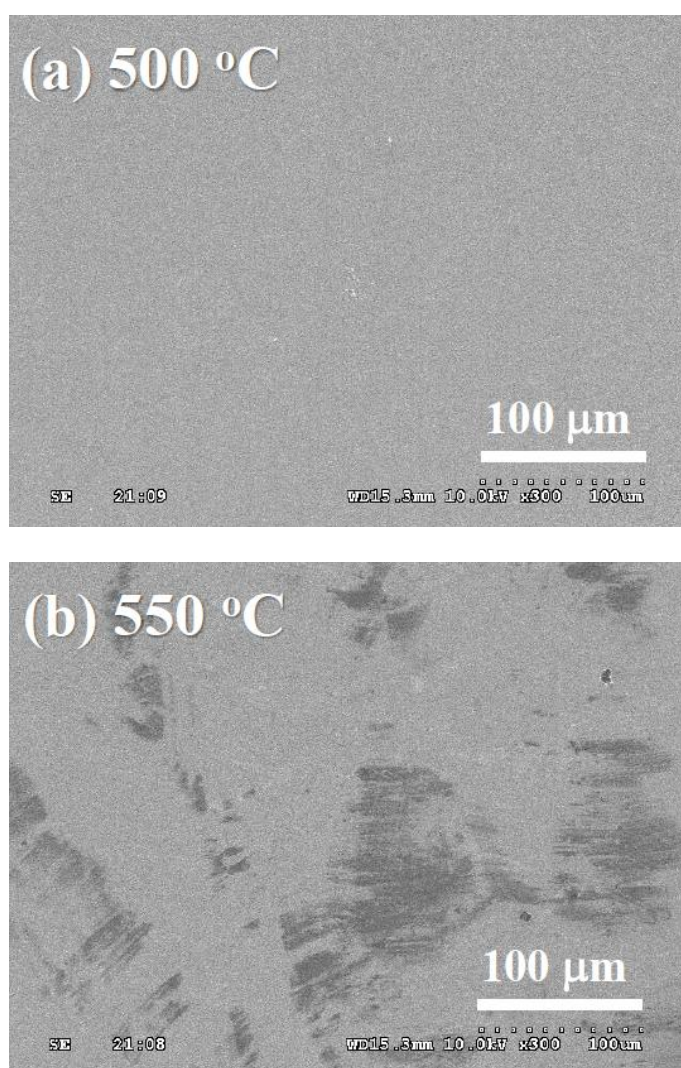


**Figure 9.** FE-SEM images of FTO substrate surface heat treated at (a) 500 °C and (b) 550 °C.

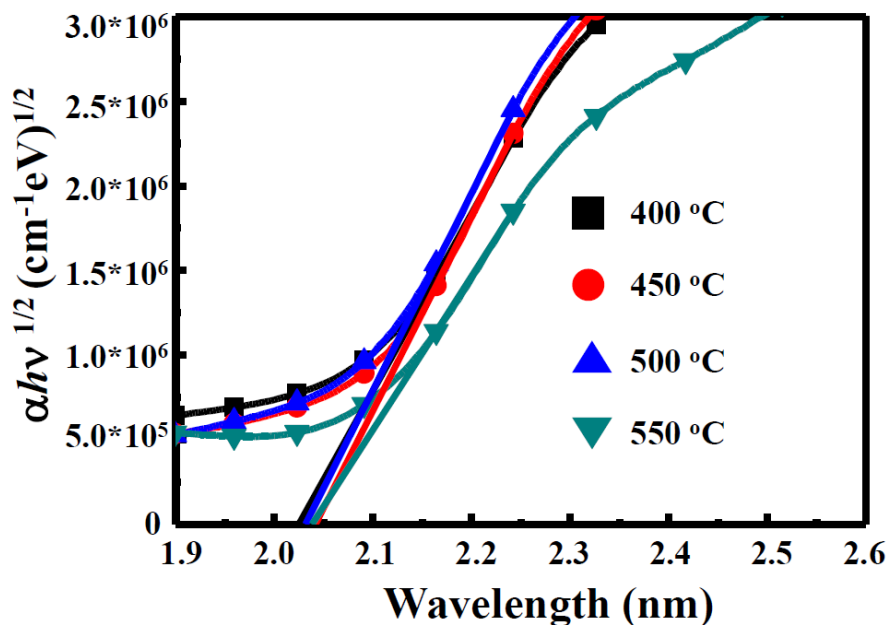


Figure 10. Plots of  $(\alpha h\nu)^{1/2}$  vs.  $h\nu$  for different heat treatment temperatures.

The  $(\alpha h\nu)^{1/2}$  vs.  $h\nu$  plot for different heat treatment temperature is shown in Fig. 10. The band gaps of  $\alpha\text{-Fe}_2\text{O}_3$  films heat treated at different temperature are found to be in the close range of 2.0-2.05 eV.

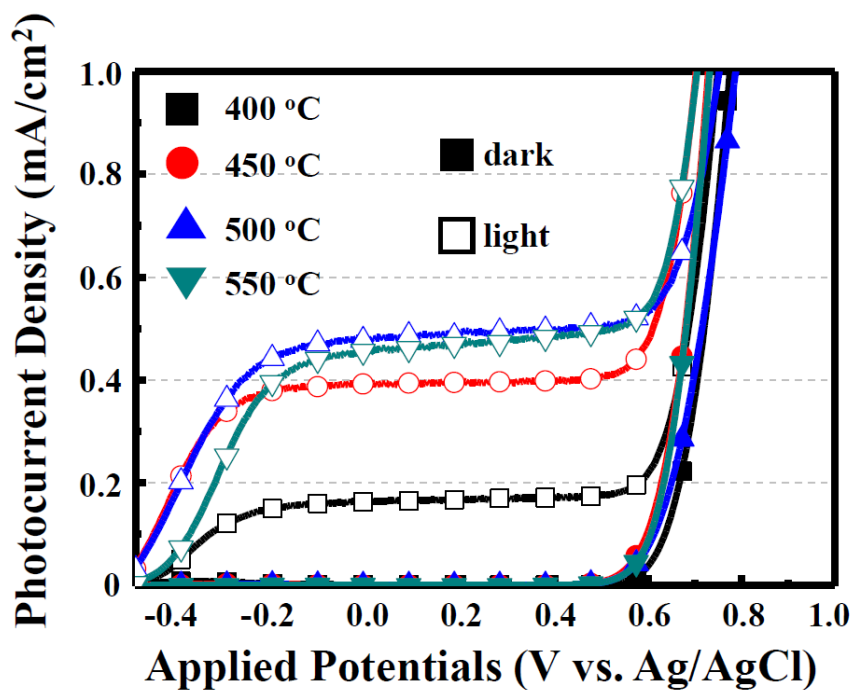
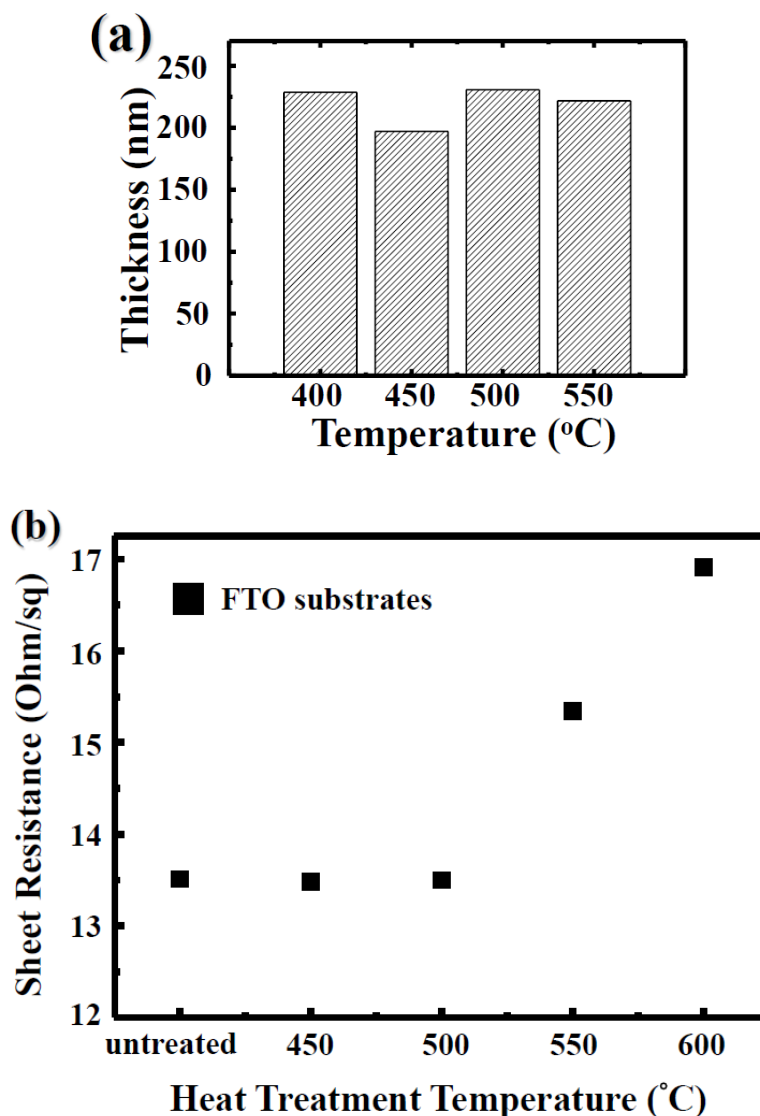


Figure 11. Photocurrent density - applied voltages plots of samples under 300 W solar simulators (AM 1.5G, 100 mW/cm<sup>2</sup>, 25°C) for different heat treatment temperatures.



**Figure 12.** (a) Thickness of  $\alpha$ -Fe<sub>2</sub>O<sub>3</sub> thin film samples heat treated at different temperatures. (b) Sheet resistances of FTO substrate heat treated at different temperatures.

Figure 11 presents photocurrent density as a function of applied potential (vs. Ag/AgCl) of the samples heat treated at different temperature in 0.5 M K<sub>2</sub>SO<sub>3</sub> + NaOH (pH = 13) electrolyte solution. The photocurrent density is 0.18 mA/cm<sup>2</sup> for the 400°C sample. It increases to 0.4 mA/cm<sup>2</sup> for the 450°C sample, and to 0.5 mA/cm<sup>2</sup> for the 500°C sample. After that, it decreases slightly to 0.48 mA/cm<sup>2</sup> for the 550°C sample. Because the film thickness for the 4 cases are very close to one another as shown in Fig. 12(a), the difference in photocurrent density is not caused by film thickness. As discussed previously, the 500°C sample has better crystallinity than 400°C and 450°C samples, and hence higher photocurrent density. For the 550°C sample, the FTO substrate is somewhat destroyed as shown in Fig. 9(b). This can be further verified by comparing the sheet resistance of FTO substrates heat treated at the various temperatures, as depicted in Fig. 12(b). The sheet resistance of unheated FTO substrate is about 13.5 Ohm/sq. It remains unchanged for temperatures up to 500°C. However, the sheet resistance increases to 15.3 Ohm/sq after being heat treated at 550 °C. This increase in

resistance of FTO substrate caused the photocurrent density to decrease. Therefore, the best heat treatment temperature for  $\alpha$ -Fe<sub>2</sub>O<sub>3</sub> film on FTO substrate is 500°C.

#### 4. CONCLUSIONS

We have successfully deposited  $\alpha$ -Fe<sub>2</sub>O<sub>3</sub> films on FTO glasses by sol-gel spin-coating technique. The crystallite grain size is found to be about 26 nm by XRD analyses. FESEM study shows worm-like morphology with nearly uniform grain distribution. The band gaps of  $\alpha$ -Fe<sub>2</sub>O<sub>3</sub> films prepared in this study are found to be in the range of 2.0-2.05 eV. By controlling the spin coating speed, heat treatment temperature and atmosphere, one can obtain a better  $\alpha$ -Fe<sub>2</sub>O<sub>3</sub> thin film for photoelectrochemical splitting of water.

#### ACKNOWLEDGEMENT

This work is partially supported by Ministry of Science and Technology and Ministry of Education of Taiwan.

#### References

1. C.-L. Tseng, C.-J. Tseng, J.-C. Chen, *Int. J. Hydrogen Energy* 35 (2010) 2781.
2. C.-H. Wang, K.-W. Cheng, C.-J. Tseng, *Sol. Energy Mater. Sol. Cells* 95 (2011) 453.
3. C.-J. Tseng, C.-H. Wang, K.-W. Cheng, *Sol. Energy Mater. Sol. Cells* 96 (2012) 33.
4. Z. Zhang, M.F. Hossain, T. Takahashi, *Int. J. Hydrogen Energy* 35 (2010) 8528.
5. C.-J. Tseng, C.-L. Tseng, *Int. J. Hydrogen Energy* 36 (2011) 6510.
6. E. Noh, K.-J. Noh, K.-S. Yun, B.-R. Kim, H.-J. Jeong, H.-J. Oh, S.-C. Jung, W.-S. Kang, S.-J. Kim, *Sci. World J.* 2013 (2013) 723201.
7. C.-Y. Chang, C.-H. Wang, C.-J. Tseng, K.-W. Cheng, L.W. Hourng, B.T. Tsai, *Int. J. Hydrogen Energy*, 37 (2012) 13616.
8. A. Fujishima, K. Honda, *Nature* 238 (1972) 37.
9. C. Santato, M. Ulmann, J. Augustynski, *Adv. Mater.* 13 (2001) 511-514.
10. M. Gupta, V. Sharma, J. Shrivastava, A. Solanki, A.P. Singh, V.R. Satsangi, S. Dass, R. Shrivastav, *Bull. Mater. Sci.* 32 (2009) 23.
11. J.H. Kennedy, K.W. Frese Jr, *J. Electrochem. Soc.* 125 (1978) 709.
12. W.B Ingler Jr, S.U.M. Khan, *Thin Solid Films* 461 (2004) 301.
13. V.R. Satsangi, S. Kumari, A.P. Singh, R. Shrivastav, S. Dass, *Int. J. Hydrogen Energy* 33 (2008) 312
14. A. Kleiman-Shwarsstein, M.N. Huda, A. Walsh, Y. Yan, G.D. Stucky, Y.S. Hu, et al., *Chemistry of Materials* 22 (2009) 510.
15. Y.-P. Hsu, S.-W. Lee, J.-K. Chang, C.-J. Tseng, K.-R. Lee, C.-H. Wang, *Int. J. Electrochem. Sci.* 8 (2013) 11615.
16. N.T. Hahn, C.B. Mullins, *Chemistry of Materials* 22 (2010) 6474.
17. W. Luo, T. Yu, Y. Wang, Z. Li, J. Ye, Z. Zou, *J. Phys. D: Appl. Phys.* 40 (2007) 1091.
18. Y. Wang, T. Yu, X. Chen, H. Zhang, S. Ouyang, Z. Li, J. Ye, Z. Zou, *J. Phys. D: Appl. Phys.* 40 (2007) 3925.

19. J.C. Manificier, M.D. Murcia, J.P. Fillard, E. Vicario, *Thin Solid Films* 41 (1977) 127.
20. M.S. Selim, A. Sawaby, Z.S.E. Mandoud, *Mater. Res. Bull.* 35 (2000) 2123.
21. X.J. Lian, X. Yang, S.J. Liu, Y. Xu, C.P. Jiang, J.W. Chen, R.L. Wang, *Appl. Surf. Sci.* 258 (2012) 2307.
22. R.A. Ismail, Y. Najim, M. Ouda, *J. Surf. Sci. Nanotech.* 6 (2008) 96.

© 2014 The Authors. Published by ESG ([www.electrochemsci.org](http://www.electrochemsci.org)). This article is an open access article distributed under the terms and conditions of the Creative Commons Attribution license (<http://creativecommons.org/licenses/by/4.0/>).